Available online at www.sciencedirect.com
ScienceDirect
Journal of Molecular Catalysis A: Chemical 280 (2008) 233–239
JOURNAL OF MOLECULAR CATALYSIS A: CHEMICAL
www.elsevier.com/locate/molcata

Gold nanocatalysts supported on protonic titanate nanotubes and titania nanocrystals

Jinhua Jiang, Qiuming Gao *, Zhi Chen

State Key Laboratory of High Performance Ceramics and Superfine Microstructures, Shanghai Institute of Ceramics, Graduate School, Chinese Academy of Sciences, 1295 Dingxi Road,Shanghai 200050, PR China

Received 9 July 2007; received in revised form 15 November 2007; accepted 15 November 2007
Available online 22 November 2007

Abstract

Gold nanoparticles were first supported on protonic titanate nanotubes with the formation of Au/titanate nanocomposites. They were further transformed to Au/titania nanocomposites via an acetic acid treatment at 70 °C for 60 h. The porosity, crystal structure and morphology of those composites have been studied by X-ray diffraction (XRD), High-resolution transmission electron microscope (HRTEM), and low-temperature nitrogen adsorption. Catalytic tests for CO oxidation show that the Au/titanate nanocomposites had a promising activity with complete conversion of CO at 70 °C and that of Au/titania was at room temperature (25 °C). Both catalysts exhibited good thermal and long-term stabilities. The influence of the crystal vacancies and surface properties of the titanate and titania supports on the catalytic activities were evaluated.

Keywords: Titanate nanotubes; Titania nanocrystals; Gold catalyst; Vacancies; OH groups

1. Introduction

Since the discovery of layered titanate nanotubes several years ago [1], intense interests have been focused on their formation mechanisms and crystalline structures [2–4]. Because of their high surface area, uniform nanotubular morphology, strong ion-exchange ability, those protonic titanate nanotubes have shown wide application in the fields of hydrogen sensors [5], hydrogen storage materials [6], Li ion batteries [7,8], enzymatic immobilization for bio-sensors [9,10], electrochromism [11], solar cell photosensitizers [12] and catalyst supports [13–15]. Recently, Zhu et al. demonstrated that this kind of nanostructures could be easily converted into titania which is one of the most important industrial metal oxides through a simple wet chemical process [16]. Our group discovered that Ni/titanate and Ni/titania can be obtained through ion-exchange method at different reduction temperatures by hydrogen flow, and studied their photocatalytic and magnetic properties [17]. Bavykin et al. reported the stability and phase transition of the titanate nanotubes in acidic, neutral, and basic aqueous suspensions [18].

Nanosized gold particles or clusters exhibited high activities for selective oxidation of hydrocarbons, water–gas shift (WGS) reaction, preferential oxidation of CO (PROX reaction), and selective epoxidation, when they were highly dispersed on oxide supports [19–21]. A series of metal oxides including TiO_2 [22–25], ZnO [25-27], Fe_2O_3 [28,29], MgO [30], Al_2O_3 [25,31], ZrO_2 [25,32] and CeO_2 [27,33,34] were successfully utilized as the supports to load gold nanoparticles and/or clusters for the CO low-temperature catalytic oxidation. Several kinds of non-oxide supports of gold nanoparticles and/or clusters, including $LaPO_4$ nanoparticles [35], $MeCO_3$ carbonates (Me = Ca, Sr, and Ba) [36], $MeCr_2O_4$ spinels (Me = Co, Mn, Fe, Mg, and Cu) [37], and carbon materials [38,39] were also explored for the CO oxidation reaction. Experimental and theoretical results show that the catalytic activity closely depends on the preparation method, pretreatment condition, gold particle diameter, support structure, metal–support interaction, and so forth [30,31,40–42]. Despite many studies on gold-based CO low-temperature catalytic oxidation, however, there is still no clear picture with respect to the origin of the catalytic activity, and many experimental results and proposed mechanisms are diverse or even contradictory. Therefore, further study is of great importance to obtain a lucid understanding of this reaction.

* Corresponding author. Tel.: +86 21 52412513; fax: +86 21 52413122.
E-mail address: qmgao@mail.sic.ac.cn (Q. Gao).

1381-1169/$ – see front matter © 2007 Elsevier B.V. All rights reserved.
doi:10.1016/j.molcata.2007.11.009

In the present study, we report the preparation of gold nanoparticles supported on protonic titanate nanotubes (abbreviated as Au/titanate) first, and subsequently via an acetic acid thermal treatment the Au/titanate catalysts were transformed into the other kind of nanocomposites, which was composed of gold nanoparticles supported on titania nanocrystals (abbreviated as Au/titania). The catalytic activity for CO oxidation was studied. The Au/titanate nanocomposites had a promising activity with complete conversion of CO at 70 °C and that of Au/titania was at room temperature (25 °C). Titanate nanotubes using as catalyst supports for esterification [13], selective oxidation of alcohols by oxygen [14], and water–gas shift reaction were reported [15]. However, no investigation on this support for the CO oxidation has been reported up to now. Here it needs to make clear that the catalysts for CO oxidation reported by Zhu et al. recently are Au/titania but not Au/titanate, which can be distinguished clearly by their sample XRD patterns. Their resulted titania (anatase phase) from the titanate precursor maintained the original one-dimensional morphology mostly [43,44]. Moreover, due to unique structural features of the titanate compared to that of titania [45,46], the correlation of the support characters between titanate and titania associated with gold-based catalysis for CO oxidation has been considered.

2. Experimental

2.1. Preparation

Titanate nanotubes were prepared under hydrothermal conditions based on Kasuga et al. [1]. 2.0 g of commercial anatase-type titanium oxides were added to 80 mL of 10 M NaOH solution under vigorous stirring. The solution was placed in a PTFE-lined stainless steel autoclave and heated to 130 °C kept for 72 h. To gain protonic titanate nanotubes the white powdery sodium titanates were first washed with dilute hydrochloric acid for 2 h and then with de-ionized water three times to remove Na^+ ions. After filtration the as-prepared hydrogen titanate nanotube samples were dried in a furnace at 80 °C for 48 h. 2.0 g of protonic titanate nanotubes were added to 80 mL of 5.0 and 2.0 mM $HAuCl_4$ solutions, respectively, stirred magnetically under exclusion of light for 24 h. The suspensions were washed with de-ionized water till the absence of Cl^- ions and recovered by filtration. The samples were dried at 80 °C and reduced under a gas flow of 5 vol% H_2 in N_2 for 2 h at 200 °C, leading to the formation of Au/titanate nanocomposites. A mount of the dark Au/titanate samples were added in an acetic acid solution with pH value of 1.5 in a reflux glass bottle, heated to 70 °C and kept for 60 h under magnetically stirring. The resulted brown precipitate was washed with de-ionized water and ethanol several times to remove CH_3COO^- ions and recovered by centrifugation. The solids were dried at 80 °C for 16 h and the Au/titania catalysts were fabricated.

2.2. Characterization

X-ray diffraction (XRD) patterns of the as-synthesized products were collected on a Rigaku D/MAX-2250V diffractmeter using Cu Kα radiation (wavelength $\lambda = 0.15147$ nm). High-resolution transmission electron microscope (HRTEM) measurements were performed on a JEM-2010 electron microscope equipped with an energy-dispersive X-ray spectroscopy (EDX) using an accelerating voltage of 200 kV for the analyses of gold contents of the catalysts. The samples were outgassed for 12 h at 240 °C to remove loosely adsorbed species. The BET surface areas and BJH pore distributions of the samples were measured using nitrogen adsorption on a Micromeritics ASAP 2020 instrument.

2.3. Catalytic reaction assays

Catalytic activities for the CO oxidation were measured in a quartz fixed-bed flow reactor under a gas mixture of 1.0 vol% CO in dry air at a flow rate of 44.6 mL/min, corresponding to a space velocity of 26.76 $Lh^{-1}g_{cat}{}^{-1}$ (using 100 mg catalyst). Prior to the measurements, all samples were in situ pretreated with an air stream at 200 °C for 1 h. The temperature was controlled by a thermocouple placed near the sample. The effluent gas was on-line analyzed with an HP-6890 gas chromatograph equipped with a thermal conductivity detector (TCD) and a molecular 13X column.

3. Results and discussion

3.1. Preparation, morphologies and structures of Au/titanate and Au/titania nanocomposites

The as-prepared protonic titanate nanotubes had uniform morphology and end-open tubular structure with outside and inside diameters of 10 and 4 nm, respectively, and interlayered space of 0.78 nm (Fig. 1a) based on the HRTEM analyses. Fig. 1b demonstrates the titania nanocrystals transformed from the protonic titanate nanotubes via an acetic acid hydrothermal treatment at 70 °C for 60 h.

EDX analyses show that the gold contents of Au/titanate and Au/titania nanocomposites were 2.60 (5.99) and 2.57 (5.91) wt%, respectively, which were prepared in the 2.0 (5.0) mM $HAuCl_4$ precursor solutions. Fig. 1c shows the resulted 5.99 wt% Au/titanate nanocomposites. After stirring and thermal treatments the supports kept their original structure basically and the Au nanoparticles were formed mainly with main size distribution of 2–5 nm and individual about 8 nm Au particles adjacent to the support margins. In a higher magnification TEM image (shown in Fig. 1d), one can observe that some of Au nanocrystals were spherical with the others elongated under the restriction of the support channels. The Au nanoparticles are supposed to be dispersed adhered to the inner- and outer-wall of the titanate nanotube supports. Hydrogen flow reduction method was chosen to prepare the nanosized gold particles. So, this method is helpful for the dispersion of gold nanoparticles both inside and outside the support tubes and enhancement of the interface areas between the metal and support, which are considered as reaction centers for CO oxidation.

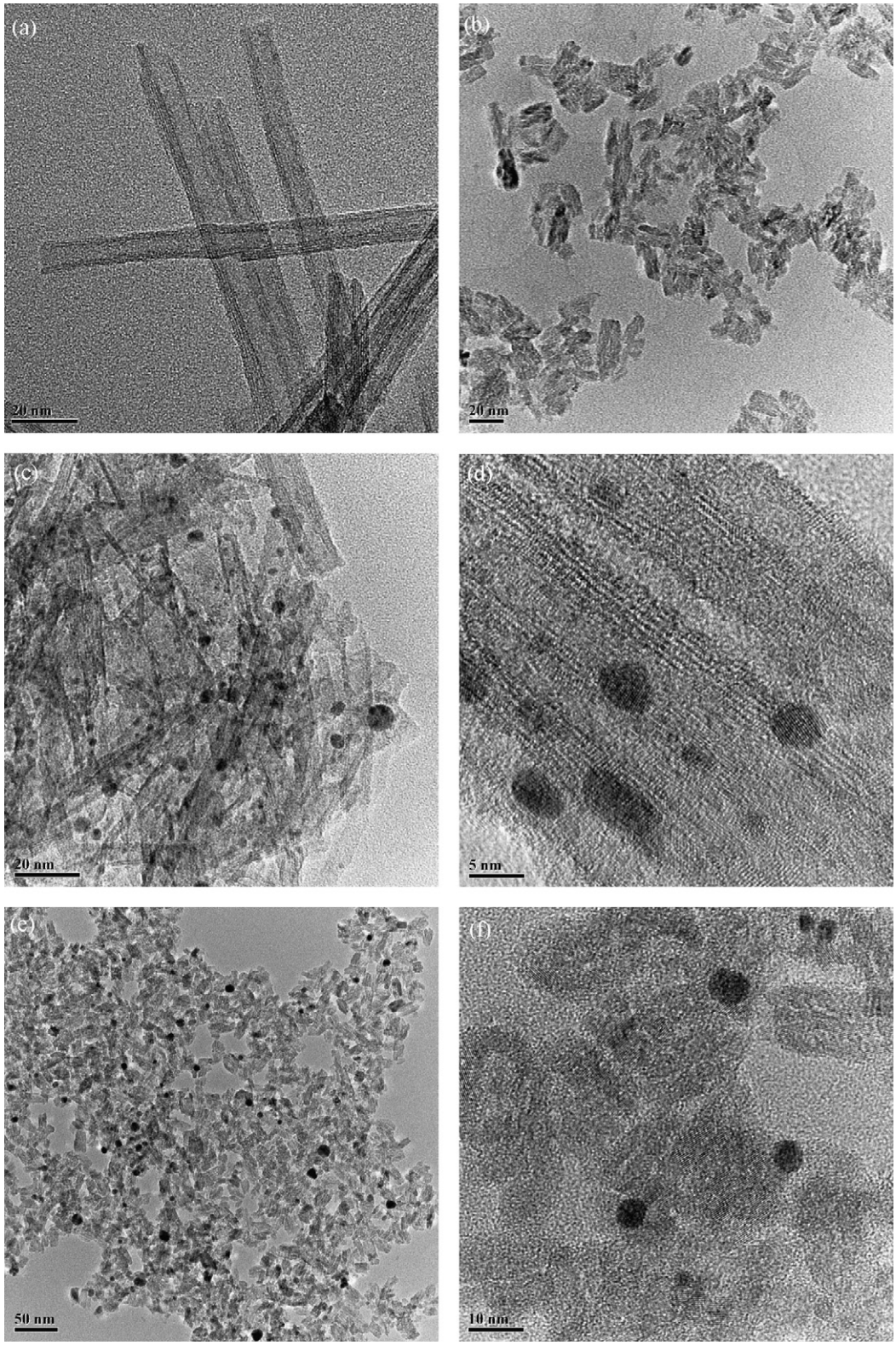

Fig. 1. HRTEM images of protonic titanate nanotubes (a), titania nanocrystals (b), 5.99 wt% Au/titanate (c) and (d) with different zooms, and 5.91 wt% Au/titania (e) and (f) with different zooms.

Representative images of the 5.91 wt% Au/titania nanocomposites are shown in Fig. 1e and f. A size growth of gold from the original 2–5 nm to the current 3–7 nm was observed and all of the Au particles were almost spherical, surrounded by the titania nanocrystals. Clearly, in this case Au particles are well encircled by the titania nanocrystals and there are sufficient interface contacts between the metal and support, which will be beneficial to the CO oxidation reaction. XRD analyses confirmed the phase

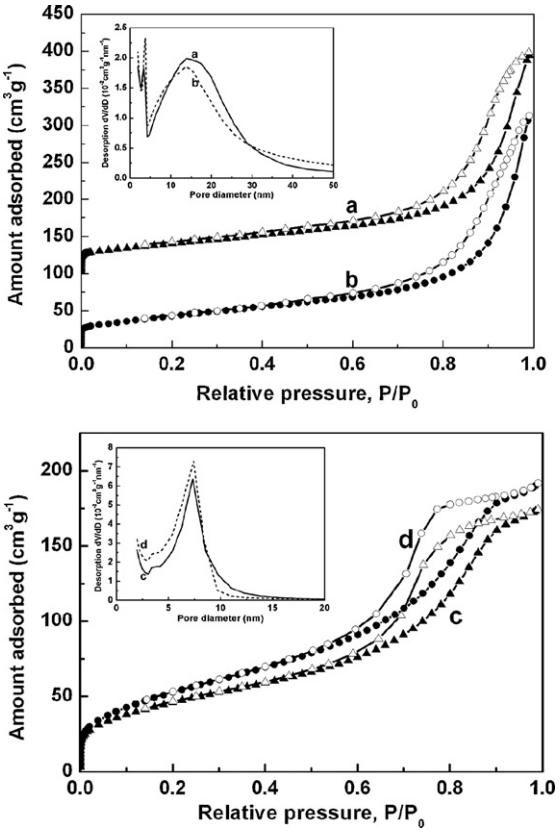

Fig. 2. Nitrogen adsorption–desorption isotherms of 5.99 wt% Au/titanate (a), 2.60 wt% Au/titanate (b), 5.91 wt% Au/titania (c), and 2.57 wt% Au/titania (d). The insets are the BJH desorption pore size distributions of these samples.

transition correspondingly, where the transformed titania was totally anatase phase (see supplementary material, Figures s1 and s2).

Low-temperature nitrogen adsorption isotherms provide detailed information on the surface area, pore volume and pore size distribution of the samples. Fig. 2 displays the nitrogen adsorption–desorption isotherms (77 K) of the 5.0 mM Au/titanate (curve a) and the resulted Au/titania (curve c), 2.0 mM Au/titanate (curve b) and the resulted Au/titania (curve d), respectively. The insets show the BJH desorption pore size distributions of those samples, correspondingly. The Au/titanate samples have the typical IV nitrogen adsorption isotherm curves based on the IUPAC classification. The BET surface areas decrease from 153 to 142 m^2/g along with the increase of gold contents from 2.60 to 5.99 wt% on the titanate supports. Both of them have two kinds of distinctive mesopores which range at 2.5–3.2 nm and 10–20 nm, respectively. Clearly, the pore structure positioned at 2.5–3.2 nm is associated with the inside pore diameters of the support titanate nanotubes, which decreased a little compared to that of the pure titanate nanotubes positioned at 3.5–4 nm. This result also confirms the incorporation of Au particles into the inner pores of the titanate nanotubes. Another pore size distribution positioned at 10–20 nm is correlated to the stacks of the tubes which similarly existed in pure titanate nanotubes [47]. The Au/titania nanocomposites also demonstrated a type IV isotherm with a sharp step characteristic of capillary condensation of nitrogen and the BET surface area decreased from 193 to 164 m^2/g along with the increase of gold contents from 2.57 to 5.91 wt% in the titania supports. There is a relatively narrow desorption pore size distribution at 5–10 nm for the Au/titania samples induced by the self-aggregation and self-accumulation of the gold and titania nanocrystals, which can be observed from the microscopic images in Fig. 1e and f. These parameters for the above-mentioned samples are summarized in Table 1.

Table 1
Textural parameters of Au/titanate and Au/titania materials

Samples	BET surface area (m^2/g)	Pore volume (cm^3/g)	BJH desorption pore size (nm)
5.99% Au/titanate	142	0.447	2.5–3.2, 10–20
2.60% Au/titanate	153	0.471	2.5–3.2, 10–20
5.91% Au/titania	164	0.267	5–10
2.57% Au/titania	193	0.292	5–10

3.2. Catalytic activity

The catalytic activities for CO oxidation by O_2 over these samples have been investigated with the increase of reaction temperatures. Fig. 3 shows the light-off curves of the 5.99 wt% Au/titanate catalysts as-prepared and after calcination in air for 2 h at 300 and 500 °C, respectively. The fresh Au/titanate sample exhibits a high activity with CO conversion of 78% at 20 °C and complete oxidization at 70 °C. After calcination treatment at 300 °C no obvious change of catalytic activities has been observed. The activities of the sample calcined at 500 °C have partly decreased with a complete conversion of CO over the temperature of 130 °C. The main reason is assigned to the gold particles growth during the high-temperature treatment, which can be reflected by the XRD patterns. At the same time the XRD diffraction peaks of the support shift slightly to high angles, owing to a severe interlayered dehydration and possible lattice distortion of the titanate nanotubes during this process (see supplementary material, Figure s3). Fig. 4 shows the light-off

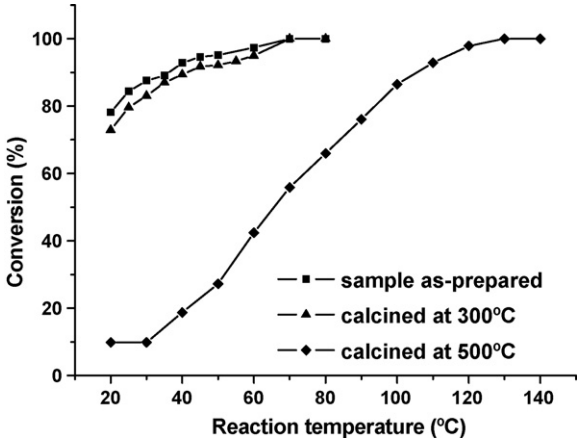

Fig. 3. CO conversion as a function of reaction temperature over 5.99 wt% Au/titanate catalysts, fresh and calcined at different temperatures.

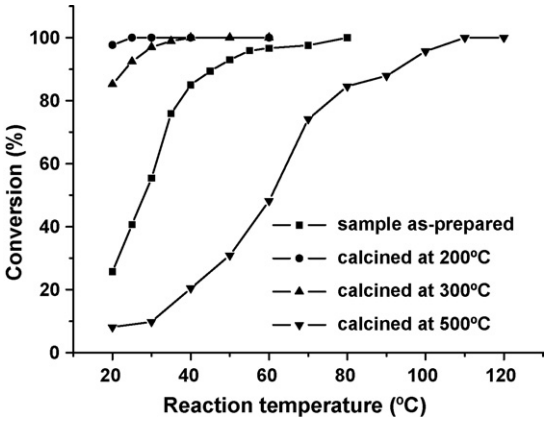

Fig. 4. CO conversion as a function of reaction temperature over 5.91 wt% Au/titania catalysts, fresh and calcined at different temperatures.

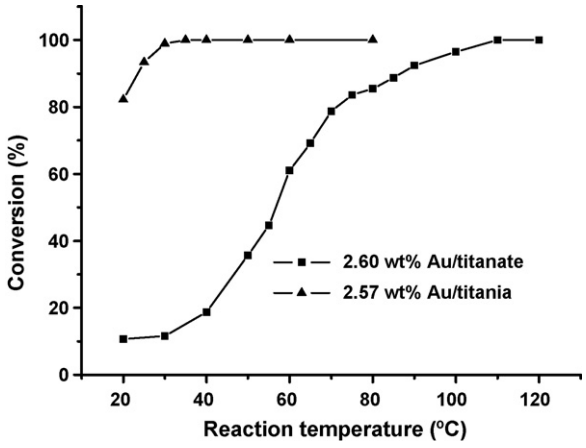

Fig. 5. Activity results over the catalysts with low gold content, 2.60 wt% Au/titanate and 2.57 wt% Au/titania.

curves of the 5.91 wt% Au/titania catalyst as-prepared, in situ calcined in air stream with flow rate of 50 mL/min at 200 °C for 1 h, calcined in air for 2 h at 300 and 500 °C, respectively. It is noteworthy that the catalytic activities of the Au/titania catalyst after calcination in air stream at 200 °C have a large enhancement compared to that of the Au/titania fresh sample. This result is different from that of the Au/titanate sample, which has no clear activity change before and after such a pretreatment process (without giving this activity curve since a large overlap with the activity curve of fresh sample in Fig. 3 for the sake of brevity). The origin of this phenomenon may be attributed to the adsorbed acetic molecules on the Au/titania catalyst surfaces during the transformation of the Au/titanate via an acid treatment and the consequent combustion of these organic species in air stream [25]. The room-temperature complete conversion of CO catalyzed by the activated Au/titania sample is stable at 300 °C and the activity loss is not very severe even after calcination at 500 °C, in agreement with the trend of the Au/titanate sample. The drop of the activity is related to the growth of the gold nanoparticles and titania nanocrystals, reflected by the XRD patterns which show sharper diffraction peaks for both of gold and titania phases after this calcination treatment (see supplementary material, Figure s4).

Catalytic activities over the 2.60 wt% Au/titanate and 2.57 wt% Au/titania samples have also been checked. Compared to the Au/titanate and Au/titania with higher gold contents, these catalysts are less active (as shown in Fig. 5). In fact, we did not observe apparent size variation of gold particles of the catalysts with different gold contents. Thus, samples with high gold content (from 5.0 mM $HAuCl_4$ precursor) possess more active areas than that of the samples with low gold content (from 2.0 mM $HAuCl_4$ precursor). We speculate they should be responsible for the differences in activity for both Au/titanate and Au/titania systems.

The catalyst activity data are summarized in Table 2, compared with some previous studies about the Au/TiO_2 system [48–51]. Generally, our samples are active at low temperature and have high specific rates, and the 2.57 wt%. Au/titania sample has the highest specific rate comparatively. However, it is difficult to make strict comparison, due to the choice of different test conditions, including temperature (T_r), $CO/O_2/N_2$ ratio, contact time, time on stream, catalyst distribution in the reactor, etc. [49].

Besides the low-temperature activity and thermal stability, as a good catalyst the long-term stability is also an important factor. Accordingly, the reaction of CO oxidation over Au/titanate and Au/titania catalysts has been tested for three consecutive cycles and then another straight 8 h. No deactivation occurred during the measurements for both of them. After stored in a close dark box at ambient atmosphere for 40 days the catalytic activities were evaluated with unchanged data. Here the Au/titania sample is also activated first in air stream at 200 °C for 1 h before activity tests, as mentioned above.

3.3. *Effect of the support structure on catalytic performances*

In fact, there are basic structure similarity between the titanate and titania that both crystal lattices consist of the octahedra sharing four edges and the zigzag ribbons [45,46]. However, differences such as elemental compositions and surface properties exist. A comparison of these two supports may provide us further understanding of the relationship between support structures and catalytic performances. As a conventional metal support for CO catalytic oxidation reaction, structure and surface properties of titania associated with the catalytic activities have been investigated thoroughly. What is generally accepted firstly is that the oxygen vacancies (the so-called F-color centers) existing in the titania can efficiently transfer charge from the support to the Au clusters thus increasing its chemical activity, which is thought to be a key factor for the activation of supported Au based on a model of SMSI (strong metal–support interaction) [30,41,52,53]. On the contrary, there is no oxygen vacancy in the titanate crystal structure, instead of vacancies of titanium, with a charge state of low electron densities. Obviously, it is impossible for the titanium vacancies of the titanate to transfer charge to the Au clusters. It is convinced that the activity of the support is sensitive to the condition of the defect sites, correlated to the Au/titanate (cation vacancies with poor

Table 2
Specific rates of CO oxidation over Au/titanate and Au/TiO_2 materials

Catalysts	Au (wt%)	T_{50} (K)[a]	T_r (K)[b]	r_{sp}(10^4 mol_{CO} s^{-1} $g_{Au}{}^{-1}$)	Refs.
Au/titanate	5.99	<293	300	0.43	This work
Au/titanate	2.60	331	300	0.12	This work
Au/titania	5.91	<293	300	0.51	This work
Au/titania	2.57	<293	300	1.1	This work
Au/TiO_2	1.8	253	300	0.31	[48]
Au/TiO_2	2.3	235	300	1.8	[48]
Au/TiO_2	3.1	235	300	6.5	[48]
Au/TiO_2	0.5	260	243	1.0	[49]
Au/TiO_2	0.35	291	243	0.8	[49]
Au/TiO_2	1.25	403	243	0.0022	[49]
Au/TiO_2	0.92	>433	243	0.03	[50]
Au/TiO_2	1	273	243	0.25	[50]
Au/TiO_2	0.16	293	243	2.0	[50]
Au/TiO_2	4.4	-	273	2.0	[51]

[a] Temperature at 50% conversion.
[b] Temperature for specific rate (r_{sp}) calculation.

electrons) and Au/titania (anion vacancies with rich electrons) systems. In addition, water can readily dissociate on titania surfaces at the oxygen vacancies to form a certain amount of OH groups [54]. These OH groups are usually proposed to be positive for the catalytic reaction [31,42]. Recent theoretical calculations through a density functional theory (DFT) study [55] have also evidenced that the high coverage of surface OH groups is helpful for O_2 adsorption and diffusion to the metal–support interface. With increase of the OH coverage, the O_2 adsorption energy is considerably enhanced. Compared to titania, protonic titanate nanotubes are totally covered on the surface by Ti-OH groups. This kind of special surface features of the protonic titanate nanotube support fully covered by OH groups should facilitate diffusion and supply of O_2 reasonably, which are considered as a rate-limiting step in such a reaction process. Finally, whether the presence of protons in the titanate supports, which renders weak acidity to the catalysts, impact on the catalytic activity is unclear for us at present.

4. Conclusions

In summary, we synthesized the Au/titanate nanocomposites through a hydrogen flow reduction of ion-exchanged titanate nanotubes in $HAuCl_4$ precursor solutions. Furthermore, Au/titania nanocomposites were obtained via an acetic acid thermal treatment of the Au/titanate. Catalytic tests of the Au/titanate sample show a high activity for CO oxidation. To the best of our knowledge, titanate nanotubes as the support of gold nanoparticles for CO oxidation have not been reported hitherto. The Au/titania sample exhibits a higher catalytic activity which converts CO completely at room temperature.

Acknowledgements

This work was financially supported by Chinese National Science Foundation (No. U0734002), Chinese Academy of Sciences (Bairen Project and Creative Foundation) and Shanghai Nanotechnology Promotion Center (No. 0652nm025). The authors thank Wei Shi for his HRTEM measurements.

Appendix A. Supplementary data

Supplementary data associated with this article can be found, in the online version, at doi:10.1016/j.molcata.2007.11.009.

References

[1] T. Kasuga, M. Hiramatsu, A. Hoson, T. Sekino, K. Niihara, Langmuir 14 (1998) 3160.
[2] Q. Chen, W.Z. Zhou, G.H. Du, L.M. Peng, Adv. Mater. 14 (2002) 1208.
[3] R.Z. Ma, Y. Bando, T. Sasaki, Chem. Phys. Lett. 380 (2003) 577.
[4] B.D. Yao, Y.F. Chan, X.Y. Zhang, W.F. Zhang, Z.Y. Yang, N. Wang, Appl. Phys. Lett. 82 (2003) 281.
[5] O.K. Varghese, D. Gong, M. Paulose, K.G. Ong, C.A. Grimes, Sens. Actuators B 93 (2003) 338.
[6] D.V. Bavykin, A.A. Lapkin, P.K. Plucinski, J.M. Friedrich, F.C. Walsh, J. Phys. Chem. B 109 (2005) 19422.
[7] J. Li, Z. Tang, Z. Zhang, Electrochem. Commun. 7 (2005) 62.
[8] L. Kavan, M. Kalbac, M. Zukalova, I. Exnar, V. Lorenzen, R. Nesper, M. Graetzel, Chem. Mater. 16 (2004) 477.
[9] A.H. Liu, M.D. Wei, I. Honma, H.S. Zhou, Anal. Chem. 77 (2005) 8068.
[10] A.H. Liu, M.D. Wei, I. Honma, H.S. Zhou, Adv. Funct. Mater. 16 (2006) 371.
[11] H. Tokudome, M. Miyauchi, Angew. Chem. Int. Ed. 44 (2005) 1974.
[12] M. Adachi, Y. Murata, I. Okada, S.J. Yoshikawa, Electrochem. Soc. 150 (2003) G48.
[13] C.H. Lin, S.H. Chien, J.H. Chao, C.Y. Sheu, Y.C. Cheng, Y.J. Huang, C.H. Tsai, Catal. Lett. 80 (2002) 153.
[14] D.V. Bavykin, A.A. Lapkin, P.K. Plucinski, J.M. Friedrich, F.C. Walsh, J. Catal. 235 (2005) 10.
[15] V. Idakiev, Z.Y. Yuan, T. Tabakova, B.L. Su, Appl. Catal. A 281 (2005) 149.
[16] H.Y. Zhu, Y. Lan, X.P. Gao, S.P. Ringer, Z.F. Zheng, D.Y. Song, J.C. Zhao, J. Am. Chem. Soc. 127 (2005) 6730.
[17] J.H. Jiang, Q.M. Gao, Z. Chen, J. Hu, C.D. Wu, Mater. Lett. 60 (2006) 3803.
[18] D.V. Bavykin, J.M. Friedrich, A.A. Lapkin, F.C. Walsh, Chem. Mater. 18 (2006) 1124.
[19] M.C. Daniel, D. Astruc, Chem. Rev. 104 (2004) 293.

[20] D. Astruc, F. Lu, J.R. Aranzaes, Angew. Chem. Int. Ed. 44 (2005) 7852.
[21] M. Haruta, T. Kobayashi, H. Sano, N. Yamada, Chem. Lett. 16 (1987) 405.
[22] M. Haruta, Catal. Today 36 (1997) 153.
[23] M. Vladen, X. Lai, D.W. Goodman, Science 281 (1998) 1647.
[24] W.F. Yan, S.M. Mahurin, Z.W. Pan, S.H. Overbury, S. Dai, J. Am. Chem. Soc. 127 (2005) 10480.
[25] M. Comotti, W.C. Li, B. Spliethoff, F. Schuth, J. Am. Chem. Soc. 128 (2006) 917.
[26] G.Y. Wang, W.X. Zhang, H.L. Lian, D.Z. Jiang, T.H. Wu, Appl. Catal. A 239 (2003) 1.
[27] G. Glaspell, L. Fuoco, M.S. El-Shall, J. Phys. Chem. B 109 (2005) 17350.
[28] M.J. Kahlich, H.A. Gasteiger, R.J. Behm, J. Catal. 182 (1999) 430.
[29] F. Boccuzzi, A. Chiorino, M. Manzoli, D. Andreeva, T. Tabakova, J. Catal. 188 (1999) 176.
[30] B. Yoon, H. Hakkinen, U. Landman, A.S. Worz, J.-M. Antonietti, S. Abbet, K. Judai, U. Heiz, Science 307 (2005) 403.
[31] M. Date, M. Okumura, S. Tsubota, M. Haruta, Angew. Chem. Int. Ed. 43 (2004) 2129.
[32] X. Zhang, H. Wang, B.Q. Xu, J. Phys. Chem. B 109 (2005) 9678.
[33] S. Carrettin, P. Concepcion, A. Corma, J.M.N. Nieto, V.F. Puntes, Angew. Chem. Int. Ed. 43 (2004) 2538.
[34] J. Guzman, S. Carrettin, J.C. Fierro-Gonzalez, Y.L. Hao, B.C. Gates, A. Corma, Angew. Chem. Int. Ed. 44 (2005) 4778.
[35] W.F. Yan, S. Brown, Z.W. Pan, M.M. Mahurin, S.H. Overbury, S. Dai, Angew. Chem. Int. Ed. 45 (2006) 3614.
[36] H.L. Lian, M.J. Jia, W.C. Pan, Yong. Li, W.X. Zhang, D.Z. Jiang, Catal. Commun. 6 (2005) 47.
[37] M. Ruszel, B. Grzybowska, K. Samson, I. Gressel, A. Klisinska, Catal. Today 112 (2006) 126.
[38] L. Prati, G. Martra, Gold Bull. 32 (1999) 96.
[39] M.M. Maye, N.N. Kariuki, J. Luo, L. Han, P. Njoki, L.Y. Wang, Y. Lin, H.R. Naslund, C.J. Zhong, Gold Bull. 37 (2004) 217.
[40] J.H. Yang, J.D. Henao, M.C. Raphulu, Y.M. Wang, T. Caputo, A.J. Groszek, M.C. Kung, M.S. Scurrell, J.T. Miller, H.H. Kung, J. Phys. Chem. B 109 (2005) 10326.
[41] M.S. Chen, D.W. Goodman, Catal. Today 111 (2006) 22.
[42] M.A. Debeila, R.P.K. Wells, J.A. Anderson, J. Catal. 239 (2006) 162.
[43] B.L. Zhu, Q. Guo, X.L. Huang, S.R. Wang, S.M. Zhang, S.H. Wu, W.P. Huang, J. Mol. Catal. A 249 (2006) 211.
[44] B.L. Zhu, Q. Guo, S.R. Wang, X.C. Zheng, S.M. Zhang, S.H. Wu, W.P. Huang, React. Kinet. Catal. Lett. 88 (2006) 301.
[45] S. Anderson, A.D. Wadsley, Acta Crystallogr. 15 (1962) 194.
[46] J.K. Burdett, T. Hughbanks, G.J. Miller, J.W. Richardson, J.V. Smith, J. Am. Chem. Soc. 109 (1987) 3639.
[47] X.M. Sun, Y.D. Li, Chem. Eur. J. 9 (2003) 2229.
[48] G.R. Bamwenda, S. Tsubota, T. Nakamura, M. Haruta, Catal. Lett. 44 (1997) 83.
[49] F. Moreau, G.C. Bond, A.O. Taylor, J. Catal. 231 (2005) 105.
[50] F. Moreau, G.C. Bond, Catal. Today 114 (2006) 362.
[51] T.V.W. Janssens, A. Carlsson, A.P. Molina, B.S. Clausen, J. Catal. 240 (2006) 108.
[52] G. Pacchioni, Chemphyschem 4 (2003) 1041.
[53] M. Sterrer, M. Yulikov, T. Risse, H.-J. Freund, J. Carrasco, F. Illas, C.D. Valentin, L. Giordano, G. Pacchioni, Angew. Chem. Int. Ed. 45 (2006) 2633.
[54] R. Schaub, P. Thostrup, N. Lopez, E. Lægsgaard, I. Stensgaard, J.K. Nørskov, F. Besenbacher, Phys. Rev. Lett. 87 (2001) 166104.
[55] L.M. Liu, B. McAllister, H.Q. Ye, P. Hu, J. Am. Chem. Soc. 128 (2006) 4017.